



Case report

HIGH-RESOLUTION MICRO-COMPUTED TOMOGRAPHY AND SCANNING ELECTRON MICROSCOPY FOR MORPHOLOGICAL ANALYSIS OF TYPE II DENS INVAGINATUS IN A MAXILLARY LATERAL INCISOR: A CASE REPORT

Miryana Raykovska¹, Hristina Tankova², Evgeni Koytchev³, Ivan Georgiev¹, Angela Gusiyska⁴.

1) *Institute of Information and Communication Technologies, Bulgarian Academy of Sciences, Sofia, Bulgaria.*

2) *Department of Pediatric Dental Medicine, Faculty of Dental Medicine, Medical University, Sofia, Bulgaria.*

3) *Institute of Mechanics, Bulgarian Academy of Sciences, Sofia, Bulgaria.*

4) *Department of Conservative Dentistry, Faculty of Dental Medicine, Medical University, Sofia, Bulgaria.*

ABSTRACT

This case report aims to present micro CT and SEM analysis of type II dens invaginatus extracted for orthodontic reasons three years after the eruption.

An industrial micro CT was used to double scan a freshly extracted left lateral incisor from the upper jaw with a peg shape and type II invagination, according to Ohlers. The first scan captured the entire tooth with a resolution of twelve micrometers, while the second scan focused on the coronal part of the tooth with a magnification of seven micrometers. This allowed for a detailed view of the overall anatomy and a reliable representation of the tooth's structure. After the scanning procedure, the tooth was sectioned, and SEM-EDS was performed on the invagination to obtain further details. Segmented image analysis provides a new detailed overview of the structural and morphological characteristics that can be observed in this type of malformation. This anatomical presentation, and SEM analysis can bring new helpful insights for practitioners and students to navigate their treatment strategies.

Keywords: Dens Invaginatus, Micro-CT, SEM, Dens in Dente,

INTRODUCTION

Dens invaginatus is a rare developmental anomaly that shows a broad spectrum of morphological variations. It affects around 0.3 - 10% of the teeth. Most frequently involved are the maxillary lateral incisors, but bilateral occurrence is not uncommon [1, 2, 3, 4, 5, 6]. The invagination results from a deepening of the enamel organ into the dental papilla prior to the calcification of the dental tissues [7]. The etiological factors that led to the appearance of this anomaly are controversial and remain unclear. Some authors suggest growth pressure of the dental arch [8], disruption of the signaling system [9], genetic influence [10, 11], and a fusion of two tooth germs [12]. The shape of the crown can also vary from entirely normal to severely deformed, and the opening to the invaginated space is usually barely noticeable [3].

Several authors have tried to describe the variability of this malformation and propose a classification [13, 14, 15]. The most widely used is suggested by Ohlers [16]. This system divides invaginations into three types determined by how far they extend radiographically from the crown to the root.

Type I: a minor enamel-lined form that does not extend beyond the amelocemental junction. Type II is an enamel-lined form that invades the root but remains limited to a blind sac. Type IIIA: Invagination extends through the root and communicates laterally with the periodontal ligament. There is usually no communication with the pulp. Type IIIB: the invagination extends through the root and communicates with the periodontal ligament.

This tooth malformation is often associated with early pulpal necrosis and subsequent periapical pathology. In most vital cases, dens invaginatus is detected by chance on the radiograph. Understanding the variable and complex internal anatomy of invaginated teeth is crucial for an adequate treatment approach. The purpose of the current case report is to present this type of morphology in a micro-CT and SEM-EDS high-resolution imaging of dens invaginatus. According to the authors, this has not been performed.

CASE REPORT

An 11-year-old girl was referred for consultation and treatment in an orthodontic clinic due to aesthetic concerns. Clinical intraoral examination revealed unilateral hypodontia. In the upper right region, tooth 12 was missing, tooth 13 erupted in its place, and tooth 52 moved in a distal direction from 13. In the upper left region, tooth 22 had an unusual peg-shaped crown. The panoramic X-ray proved the absence of tooth germ 12 and indicated an invagination of tooth 22, lined by enamel-like radiodensity that remains close to the pulp chamber (Fig. 1). No other structural defects were established. Tooth 22 was tested and proved vital, and there was no periapical radiolucency.

Fig. 1. Orthopantomographic pretreatment image of the patient. Invagination is visible on tooth 22.



The parents haven't reported any complications during pregnancy, and the girl had no history of orofacial trauma. There was no history of such unilateral hypodontia in the family and no history of dens invaginatus.

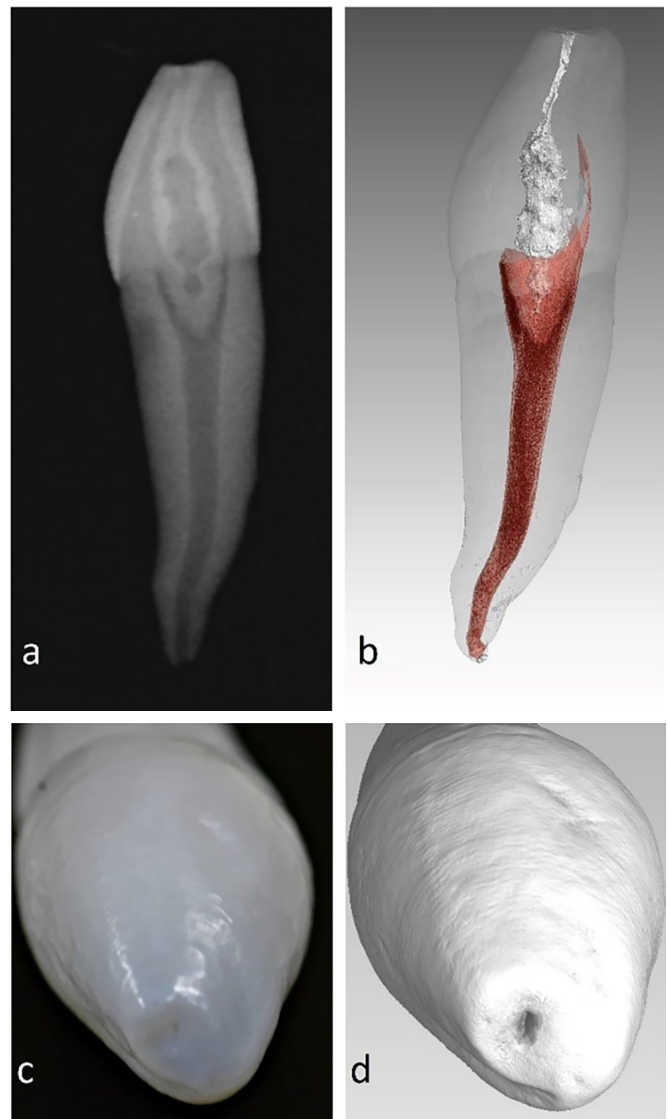
Written informed consent was obtained, and tooth 22 was extracted for orthodontic reasons after careful observation of the clinical and radiological findings. Parents also signed a declaration certifying their consent to the tooth examination.

After the extraction, the tooth was cleaned and stored in HBSS (Hanks' Balanced Salts - Capricorn Scientific Germany) in order to prevent dehydration and changes in the mineral composition, and it was submitted for investigation.

The tooth examination was performed in three stages: two micro-CT examinations with different resolutions and an SEM-EDS examination.

The first scan was performed on the entire tooth. The scan was done by means of Nikon XT H 225 (Nikon Metrology, UK), the X-ray parameters were a voltage of 94 kV and a current of 101 μ A. A Series of 2520 projections with one frame per projection, an exposure time of 708 ms, and an isotropic resolution of 12 μ m per voxel were acquired during a continuous rotation range of 360°. The images were reconstructed with CT Pro 3D (version XT 3.1.3, Nikon Metrology, Hertfordshire, UK), using a beam hardening correction and noise reduction preset with index number "three" and a median filter with a kernel size of 3X3.

Fig. 2. Comparative image of the sample post extraction a) x-ray image of the hole invaginated tooth after the extraction, b) the rendered image after the first micro-CT scan with the same orientation and resolution of 12 microns, c) macro photographic shoot of the coronal foramen of the invagination and d) three dimensional rendered image of the coronal foramen after the first scan.



Three-dimensional models were generated on VG Studio MAX (version 2.2, Volume Graphics, Germany) to visualize the tooth's overall anatomy. The invagination and the canal of the tooth were segmented with the region-growing method after the closure of the apical and coronal foramen with a digital pen. (Fig. 2).

The second scan was done only on the invaginated part, with the same hardware and software but corrected parameters - voltage of 92kV and a current of 104μA. A series of 2520 projections with two frames per projection, an exposure time of 708ms, and an isotropic resolution of 7μm per voxel.

In the third part of the research, the coronal part of the tooth with the invagination was sliced, and new samples were created. After dehydration protocol in alcohol with rising concentration for twenty-four hours, the samples were coated with a gold sheet. SEM analyzed the morphology and elemental composition with an energy dispersive analyzer on a JEOL JSM 6390 equipped with an INCA Oxford energy dispersive (EDS) detector. The accelerating voltage was 20 kV, and the probe current was 1 pA to 1 uA.

After the reconstruction and segmentation procedure, several measurements were done. The analysis begins from the coronal opening. The form of the coronal foramen is elliptical (Fig. 2) with dimensions 0.23mm to

0.42mm. It passes inwards into a channel that narrows to an approximate length of 2.6mm. This channel has a diameter of 0.23mm by 0.12mm in its narrowest part. In the apical direction, the invagination expands and acquires a spherical shape with many protrusions. From the coronal foramen to the end below the level of the enamel-cement border, the total length of this structure is approximately 8.15mm, and the width varies between 1mm and 1.36mm. The thickness of the enamel in the invagination also varies in width, mostly about 3-4mm, and in some areas between 0-5mm.

After the second scan, large amounts of tubular (porous) formations, like additional invaginations located on the enamel wall of the main invagination, were visualized and segmented. More than 70 of these formations were counted. They are only in the bulbous part of the invagination, and the shape is almost cylindrical. Those tubules extend the entire thickness of the invaginated enamel perpendicular to the central axis of the main invagination. Some end closed with enamel, but others open directly in contact with dentin tubules. The diameter of these channels is less than 0.1mm, varying between 0.09mm for the widest and 0.030mm for the smallest. In some areas, the proximity between the tubules opening directly into the dentin and the pulp chamber is significant; 0.217mm was the smallest detected (Fig. 3, Fig. 4).

Fig. 3. Microtomographic image post-extraction, after the second scan: a) sagittal section of the invagination, b) horizontal section of the invagination, c) rendered image - blue is the segmented space in the invagination, red is the pulp space, and in green are the dead tracts in the dentin. In each image, the dead tracts are enlarged and brought to the side. Additional channels are indicated with an arrow, an asterisk marks tissue with weak X-ray contrast in the invagination cavity, and a circle indicates an area of the invaginated enamel where a decrease in the intensity of enamel grey is visible.

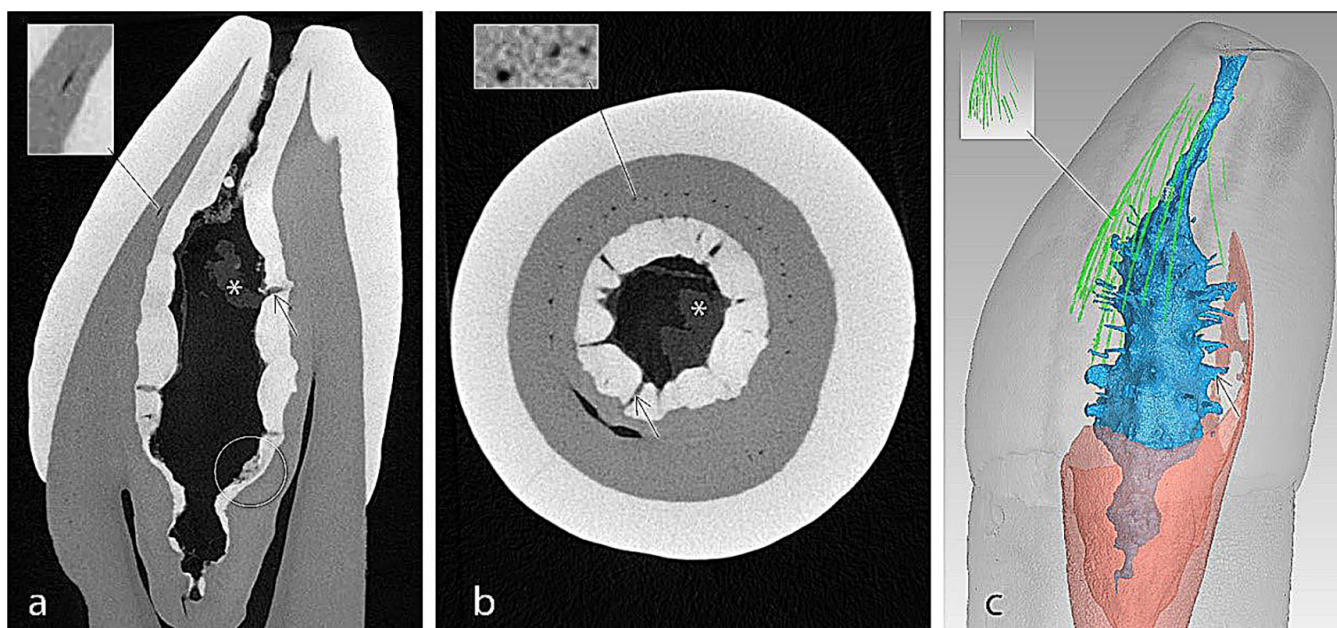
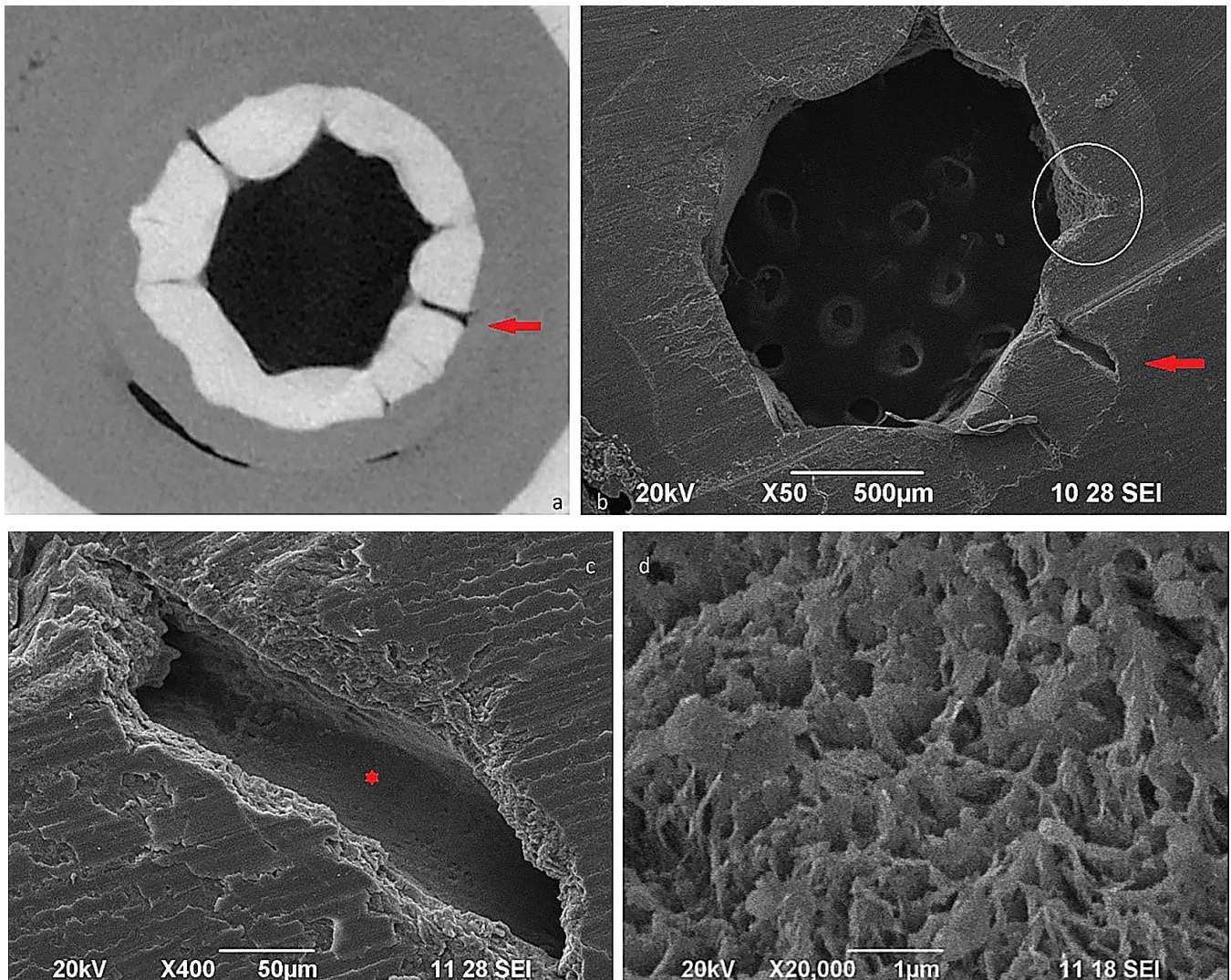


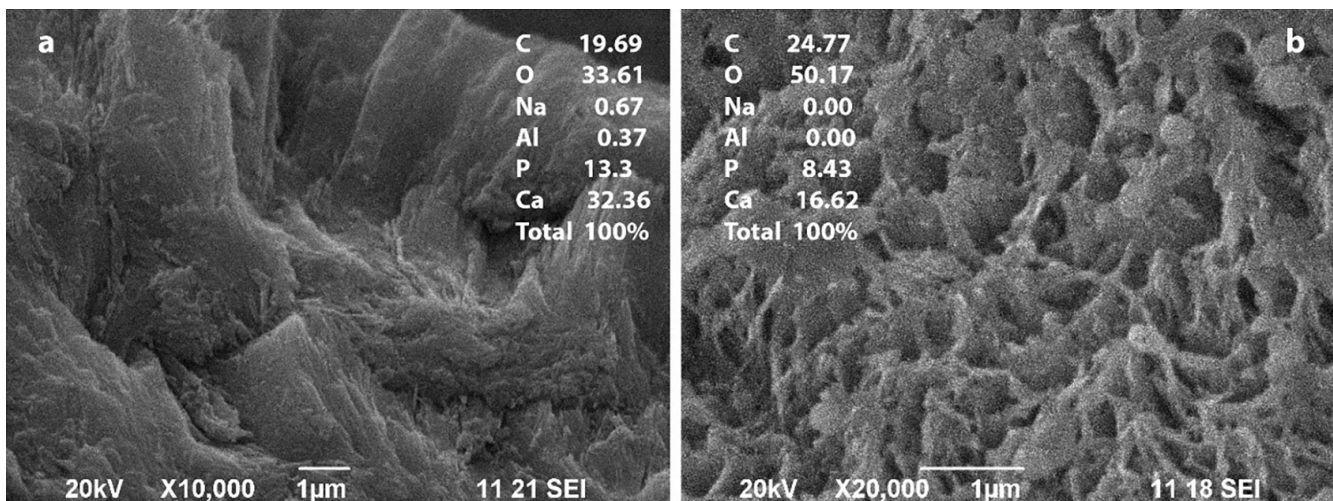
Fig. 4. Combining micro-CT and SEM images demonstrates a picture of the same section a), b). A red arrow in both images indicates the additional indentation in the form of a groove and the next magnification point. In picture a), it is visible that the groove opens directly in dentin, and picture b), a white circle indicates a section where an accumulation of bacterial mass is observed. c) The canal-like intussusception is magnified 400 times, and an asterisk marks the point of the next magnification. d) The enamel prism at the last magnification point.



The position of the peaks in the resulting diagram of the spectrum after the SEM investigation corresponds to the concentration of the element. Five specimens were examined, and a complete additional invagination channel was detected in only one sample. EDS analysis of each sample was carried out in the following areas: outer enamel, invaginated enamel, additional invagination enamel and dentin. Significant differences in enamel mineral content were detected only between the invaginated enamel and the enamel in the accessory invaginations. There was no significant difference between outer and invaginated enamel.

The amount of calcium and phosphorus in the additional tubule is almost half compared with the enamel of the crown. The structure of this inner enamel prism is also visibly immature (Fig. 5).

Fig. 5. Comparative SEM and EDS analysis between the invaginated enamel layer and the enamel layer in the additional invaginations. The values from the EDS analysis are represented numerically for each image respectively.



DISCUSSION

Dens invaginatus is a dental anomaly that has been studied in various populations [1, 2, 3, 4, 5, 6]. However, none of these studies have reported a case where a patient has unilateral dens invaginatus and hypodontia of the same tooth in the other quadrant. Teeth with invagination can usually be saved, but in this case, the unique combination with hypodontia requires complex orthodontic and prosthodontic treatment, including extraction of the affected tooth. This case report results from the opportunity to examine the extracted tooth with the modern capabilities of micro-CT digitizing and segmenting images, combined with the detail of scanning electron microscopy.

The exact cause of the invagination is unknown. However, early detection is crucial for preserving the vitality of the teeth. In most cases, such as the one presented in this report, dens invaginatus is identified by chance during a radiograph. In this particular case, the malformation was detected three years after the tooth had erupted.

At the top of the peg-shaped crown is an opening of the invagination that extends and forms a channel. The measurements on the digitized and rendered image of this malformation show that it is possible to examine it with a small k-file (number 10) for diagnosis and differential diagnosis.

Upon observing a detailed anatomical presentation, clear signs of bacterial invasion along with initial demineralization were noticed. Micro-CT images (Fig. 3) revealed freely “floating” matter in the bulbous part of the invagination, indicating the possibility of bacterial invasion. The grey value, which represents the mineral content of this floating matter, is much lower than the rest of the mineralized structures. The mean threshold for this floating matter is 50, while

the mean threshold of the dentin (as less mineralized) on the same image is 126 out of 256 shades (8-bit image). Additionally, all of the SEM images showed bacterial mass layered on the wall of the invaginated enamel. There have been some findings regarding the early stages of tooth demineralization. One of these findings is the visible thinning of the enamel at the tip of the invagination, with some areas showing complete enamel loss. Additionally, a zone on the enamel (Fig. 3) has lower grey values when compared to the surrounding enamel.

During the second scan, the anatomy was examined thoroughly with high resolution, leading to the discovery of more than 70 additional invaginations. Some of these invaginations end in enamel while others open in dentin. Similar structures have been described or observed in other articles, which indicates that this is not an isolated case [17, 18, 19, 20]. A comparative image was established using micro-CT and SEM, which confirmed the anatomy while providing details on mineral content and microstructural features (Fig.4). However, the proximity between the pulp chamber and the additional enamel tubules creates a risk of rapid invasion and inflammation of the pulp space.

To the best of our knowledge, there is a previously undocumented feature regarding the structure of the enamel prisms and their mineral content in the additional tubules. SEM-EDS analysis revealed that the mineral content of the tubules is significantly lower than that of the remaining enamel in the invagination (Fig. 5). There is an interesting similarity between the images and the results in this study and those reported by Chaudhary *et al.* [21] in their article on artificial enamel demineralization, which also included SEM-EDS analysis. However, there was no discernible difference in the mineral composition of the coronary and invaginated enamel,

as reported by Mishra *et al.* [16] in their case report. Additionally, the enamel appears immature, but there is no visible bacterial invasion in the examined area (Fig. 4, Fig. 5). The amount of calcium and phosphorus is almost half in the enamel of the additional tubule compared to the outer enamel.

Using advanced technology and a resolution of 7 microns, we were able to detect and segment dead tracts in dentin with a high degree of accuracy using micro-CT images. This allowed us to visualize these tracts in three dimensions, providing a much more detailed and comprehensive view of the structure of dentin. This breakthrough has the potential to significantly enhance our understanding of the structure and function of dentin.

Acknowledgement:

The authors would like to express their gratitude for the financial support of the Bulgarian National Science Fund, grants KP-06-H27/6 from 08.12.2018.

REFERENCES:

1. Capar ID, Ertas H, Arslan H, Tarim Ertas E. A retrospective comparative study of cone-beam computed tomography versus rendered panoramic images in identifying the presence, types, and characteristics of dens invaginatus in a Turkish population. *J Endod.* 2015 Apr;41(4):473-478. [[PubMed](#)]
2. Hamasha AA, Alomari QD. Prevalence of dens invaginatus in Jordanian adults. *Int Endod J.* 2004 May;37(5):307-310. [[PubMed](#)]
3. Kfir A, Flaisher Salem N, Natour L, Metzger Z, Sadan N, Elbahary S. Prevalence of dens invaginatus in young Israeli population and its association with clinical morphological features of maxillary incisors. *Sci Rep.* 2020 Oct 13;10(1):17131. [[PubMed](#)]
4. Mabrouk R, Berrezouga L, Frih N. The Accuracy of CBCT in the Detection of Dens Invaginatus in a Tunisian Population. *Int J Dent.* 2021 Jan 25;2021:8826204. [[PubMed](#)]
5. Alkadi M, Almohareb R, Mansour S, Mehanny M, Alsadhan R. Assessment of dens invaginatus and its characteristics in maxillary anterior teeth using cone-beam computed tomography. *Sci Rep.* 2021 Oct 5;11(1):19727. [[PubMed](#)]
6. Chen L, Li Y, Wang H. Investigation of dens invaginatus in a Chinese subpopulation using Cone-beam computed tomography. *Oral Dis.* 2021 Oct;27(7):1755-1760. [[PubMed](#)]
7. Hülsmann M. Dens invaginatus: aetiology, classification, prevalence, diagnosis, and treatment considerations. *Int Endod J.* 1997 Mar;30(2):79-90. [[PubMed](#)]
8. Segura JJ, Hattab F, Ríos V. Maxillary canine transpositions in two brothers and one sister: associated dental anomalies and genetic basis. *ASDC J Dent Child.* 2002 Jan-Apr;69(1):54-12. [[PubMed](#)]
9. Ohazama A, Courtney JM, Sharpe PT. Opg, Rank, and Rankl in tooth development: co-ordination of odontogenesis and osteogenesis. *J Dent Res.* 2004 Mar;83(3):241-4. [[PubMed](#)]
10. Hosey MT, Bedi R. Multiple dens invaginatus in two brothers. *Endod Dent Traumatol.* 1996 Feb;12(1):44-7. [[PubMed](#)]
11. Pokala P, Acs G. A constellation of dental anomalies in a chromosomal deletion syndrome (7q32): case report. *Pediatr Dent.* 1994 Jul-Aug;16(4):306-9. [[PubMed](#)]
12. Bruszt P. [Etiology of dens in dente]. [in German] *SSO Schweiz Monatsschr Zahnheilkd.* 1950 Jun;60(6):534-42. [[PubMed](#)]
13. Ulmansky M, Josef Hermel J. Double dens in dente in a single tooth: Report of a case and radiologic study of the incidence of small dens in dente. *Oral Surg Oral Med Oral Pathol.* 1964 Jan;17:92-7. [[PubMed](#)]
14. Vincent-Townend J. Dens invaginatus. *J Dent.* 1974 Nov;2(6):234-8. [[PubMed](#)]
15. Schulze C, Brand E. [Dens invaginatus (dens in dente)]. [in German] *ZWR.* 1972 Jul 25;81(14):653-60 contd. [[PubMed](#)]
16. Oehlers FA. Dens invaginatus (dilated composite odontome). I. Variations of the invagination process and associated anterior crown forms. *Oral Surg Oral Med Oral Pathol.* 1957 Nov;10(11):1204-18. [[PubMed](#)]
17. Greco ACDL, Azevedo CD de B e, Cardoso CA e A, Cardoso FO, Rios MMNS, Simoes NM, et al. A clinical case report of dens in dente in an unusual location. *J Oral Diagn.* 2017 Jan 5;2:1-4. [[Crossref](#)]
18. Rajasekharan S, Martens L, Vanhove C, Aps J. In vitro analysis of extracted dens invaginatus using various radiographic imaging techniques. *Eur J Paediatr Dent.* 2014 Sep;15(3):265-70. [[PubMed](#)]
19. Mishra S, Mishra L, Sahoo SR. A Type III Dens Invaginatus with Unusual Helical CT and Histologic Findings: A Case Report. *J Clin Diagn Res.* 2012 Nov;6(9):1606-9. [[PubMed](#)]
20. Alani A, Bishop K. Dens

CONCLUSION

Based on our findings, it can be concluded that dens invaginatus of the second type may have multiple additional invaginations in the enamel wall of the main invagination. This increases the risk of bacterial invasion of the dentin and pulp, which may lead to early stages of pulp inflammation. However, despite this risk, the tooth may still be vital for up to three years after eruption. It is important to carefully consider treatment strategies when dealing with this condition, taking into account the possibility of pulp inflammation and its early detection.

invaginatus. Part 1: classification, prevalence and aetiology. *Int Endod J.* 2008 Dec;41(12):1123-1136. [PubMed]

21. Chaudhary I, M Tripathi A, Yadav G, Saha S. Effect of Casein Phosphopeptide-amorphous Calcium Phosphate and Calcium Sodium Phosphosilicate on Artificial Carious Lesions: An *in vitro* Study. *Int J Clin Pediatr Dent.* 2017 Jul-Sep;10(3):261-266. [PubMed]

Please cite this article as: Raykovska M, Tankova H, Koytchev E, Georgiev I, Gusiyska A. High-resolution Micro-Computed Tomography and Scanning Electron Microscopy for Morphological analysis of Type II Dens Invaginatus in a Maxillary Lateral Incisor: A case report. *J of IMAB.* 2024 Oct-Dec;30(4):5888-5894. [Crossref - <https://doi.org/10.5272/jimab.2024304.5888>]

Received: 30/08/2024; Published online: 04/12/2024



Address for correspondence:

Miryana Raykovska, DDS, MSc,
Institute of Information and Communication Technologies, Bulgarian Academy
of Sciences;
Acad. G. Bonchev Str. bl. 2, 1113 Sofia, Bulgaria,
E-mail: mirianaraykovska@gmail.com,